Blind Detection for MIMO Systems With Low-Resolution ADCs Using Supervised Learning

Yo-Seb Jeon, Song-Nam Hong, and Namyoon Lee

arXiv:1610.07693v2 [cs.IT] 26 Oct 2016

***Abstract*—This paper considers a multiple-input-multiple-output (MIMO) system with low-resolution analog-to-digital converters (ADCs). In this system, we present a novel blind detection framework that performs data symbol detection without explicitly knowing channel state information at a receiver. The underlying idea of the proposed framework is to exploit supervised learning. Specifically, during channel training, the proposed approach sends a sequence of data symbols as pilots so that the receiver learns a nonlinear function that is determined by both a channel matrix and a quantization function of the ADCs. During data transmission, the receiver uses the estimated nonlinear function from labeled training data to detect which data symbols were transmitted. We propose three blind detection methods, which are connected to a K-nearest neighbors classification and a nearest-centroid classification. We also provide an analytical expression for the symbol-vector-error probability of the MIMO systems with one-bit ADCs when employing the proposed framework. One major observation is that the symbol-vector-error probability decreases exponentially with the inverse of the number of transmit antennas, the operating signal-to-noise ratio, and the minimum distance that can increase with the number of receive antennas. Simulations demonstrate the performance improvement of the proposed framework compared to existing detection techniques.**

***Index Terms*—Multiple-input-multiple-output (MIMO) detection, noncoherent detection, analog-to-digital converter (ADC), one-bit ADC, supervised learning, classification.**

I. Introduction

Future wireless systems (e.g. mmWave systems) are possible to provide communication links with Gbps data rates by using wide bandwidths. As the system bandwidth increases, the sampling rate of an analog-to-digital converter (ADC) should increase linearly with the bandwidth. Unfortunately, the higher sampling rate gives rise to the larger power consumption of the ADC, and it turns out that the power consumption scales linearly with both precision level and sampling rate [1], [2]. Therefore, the use of the ADCs with a few-bit precision has been regarded as a cost-effective solution to reduce power consumption of devices that use high-speed ADCs. For example, there has been a lot of interests to use one-bit ADCs, because they significantly reduce not only power consumption but also hardware cost (e.g., automatic gain control is not required for one-bit ADCs).

When low-resolution ADCs are used in communication systems, the characterization of the channel capacity is challenging, because a received signal is significantly distorted by nonlinear quantization operation at the ADCs. In a simple case in which one-bit ADCs are used in a single-input-single-output (SISO) system, the system capacity has been extensively analyzed [1]–[5]. For instance, it has shown in [4] that quadrature-phase-shift-keying (QPSK) modulation is optimal in an information-theoretical sense.

Recently, multiple-input-multiple-output (MIMO) systems with low-resolution ADCs have received great attentions because the use of multiple antennas has a potential to increase spectral efficiencies of wireless communications [6]–[8]. When low-resolution ADCs are used in MIMO systems, however, the characterization of the channel capacity is much more complicated than in SISO systems, and the exact capacity expression is not known in general. For the one-bit quantized MIMO channel, the channel capacity has been analyzed under the premise that channel state information at a transmitter (CSIT) and channel state information at a receiver (CSIR) are perfect and that signal-to-noise ratio (SNR) is extremely high [6]. In addition to the capacity analysis, to realize the potential diversity and multiplexing gains of MIMO systems, numerous detection methods have also been proposed for the MIMO systems with the low-resolution ADCs [9]–[14]. For example, linear-detection methods have been developed for high-order-modulation input signals when a least-squares (LS) method is used to estimate the MIMO channel [10], and a near maximum-likelihood (ML) detector that uses a convex optimization technique has been proposed for the MIMO systems that use one-bit ADCs [14].

Most existing MIMO detection techniques have been developed under the assumption of estimated or perfect CSIR, to perform coherent detection. In the MIMO system with the low-resolution ADCs, however, accurate CSIR cannot be readily obtained from pilot signals due to the coarse quantization that is applied when receiving signals. To resolve this problem, several channel estimation methods have been developed to improve the accuracy of CSIR [14]–[16]. The common problem of the methods is that they require a huge amount of the pilot signals. Furthermore, at high SNR, the mean-square error of the LS channel-estimation method degrades significantly [16].

Blind MIMO communications have been studied by some researchers to provide the gains of MIMO systems, even when accurate CSIR is not available. The capacity of blind MIMO communication systems with perfect (infinite precision) ADCs has been thoroughly analyzed on the basis of the Grassmanian manifold, where block-fading channels are assumed [17]. For the data detection of such systems, semi-blind MIMO detection methods, which perform channel estimation and data

Y.-S. Jeon and N. Lee are with the Department of Electrical Engineering, POSTECH, Pohang, Gyeongbuk, 37673 Korea (e-mail: jys900311@postech.ac.kr, nylee@postech.ac.kr).

S.-N. Hong is with the Department of Electrical Engineering, Ajou University, Suwon, Korea (e-mail: snhong@ajou.ac.kr).

detection jointly, have been developed and shown to achieve a superior performance compared to the coherent detection methods for certain scenarios (e.g. very low SNR) [18]–[23]. Completely-blind MIMO detection techniques have also been developed using the K-means clustering algorithm [22] and decision-feedback differential detection [23]. Unfortunately, these blind techniques are only available for a particular type of modulation, e.g., space-shift-keying modulation [22] and phase-shift-keying (PSK) modulation [23]. The most relevant prior work that considers the use of low-resolution ADCs with the blind MIMO detection is a joint channel-and-data estimation method in [12] developed by using Bayesian inference theory. This method, however, has high implementation complexity, which may not be affordable in practical communication systems.

In this paper, we propose a novel blind detection approach for the MIMO system with low-resolution ADCs when explicit CSIR is not known to a receiver. The proposed approach consists of two phases. In the first phase, the transmitter sends a sequence of data symbols so that the receiver learns a nonlinear function that describes input-output relations of the system, which is determined by both a channel matrix and a quantization function of the ADCs. In the second phase, using the estimated nonlinear function, the receiver detects the data symbols, which essentially does not require explicit CSIR. This new approach is closely connected to a classification problem in supervised learning. The index of a transmitted symbol vector and the received signal vector can be regarded as a class label and the associated feature vector, respectively. With the lens of supervised learning, therefore, developing a detection method for a MIMO system is equivalent to designing a classifier that maps the received signal to one of the indexes of possible symbol vectors.

We summarize our contribution as follows:

- Using this new approach, we first propose two channel-training methods to learn the nonlinear MIMO channel with a simple repetition transmission of all possible symbol vectors. Specifically, the common idea of the proposed channel-training methods is to learn an empirical conditional probability mass function (PMF) for each symbol vector, which provides statistical information about the received signals for a given symbol vector. Using this PMF, in the data transmission phase, we introduce three blind MIMO detection methods; 1) Empirical Maximum-Likelihood Detection (eMLD), 2) Minimum-Mean-Distance Detection (MMD), and 3) Minimum-Center-Distance Detection (MCD), and explain how they are related to well-known classification algorithms such as a K-nearest neighbors (KNN) classifier and a nearest-centroid classifier (NCC).
- We analyze the symbol-vector-error probability for the MIMO systems that use one-bit ADCs and binary-phase-shift-keying (BPSK) modulation. Particularly, by regarding all possible received vectors as codewords of a nonlinear code, we derive the upper bound of the symbol-vector-error probability for a fixed channel matrix, which is characterized in terms of the minimum Hamming distance $d_{\min}$ of the code. One major observation is that the symbol-vector-error probability decreases exponentially with the inverse of the number of transmit antennas, the operating SNR, and the minimum distance that can increase with the number of receive antennas. To provide a more clear understanding for the error performance under a random channel realization, we derive the approximate distribution of $d_{\min}$, assuming Rayleigh-fading channels. In particular, for the case of $N_{\rm t} = 2$, we provide an exact distribution of $d_{\min}$. Our analysis results show that $d_{\min}$, indeed, increases linearly with $N_{\rm r}$.
- We evaluate the performance gains of the proposed blind detection techniques compared to existing detection techniques, using simulations. Simulation results show that as SNR increases, the proposed detection techniques achieve symbol-error rates (SERs) that are comparable to the SER of the ML detection method with perfect CSIR, even when the training sequence is very short. Simulation results also show that our approach provides a significant SER reduction as the number of ADC bits increased. For example, by simulation, we demonstrate that the ADCs with 3-bit resolution are sufficient for the proposed techniques to obtain SER near to the perfect-ADC case with channel estimation. In addition to the performance evaluation, we also show the validation of the analysis by simulations.

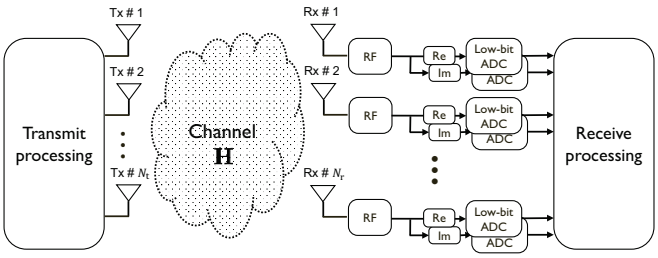

Fig. 1. Illustration of a MIMO system with low-resolution ADCs that are applied separately to the real and imaginary part.

Notation: Upper-case and lower-case boldface letters denote matrices and column vectors, respectively. $\mathbb{E}[\cdot]$ is the statistical expectation, $\mathbb{P}(\cdot)$ is the probability, $(\cdot)^\top$ is the transpose, $(\cdot)^H$ is the conjugate transpose, $|\cdot|$ is the absolute value, $\mathrm{Re}(\cdot)$ is the real part, $\mathrm{Im}(\cdot)$ is the imaginary part, and $\lfloor\cdot\rfloor$ is the floor function. $\mathbf{I}_m$ is an $m \times m$ identity matrix, and $\mathbf{0}_n$ is an n-dimensional all-zero vector, $\mathcal{N}(\mu, \mathbf{R})$ and $\mathcal{CN}(\mu, \mathbf{R})$ represent the distributions of real and circularly-symmetric complex Gaussian random vector, respectively, which have the mean vector μ and covariance matrix $\mathbf{R}$.

II. System Model

In this section, we present a system model for a MIMO system with low-resolution ADCs.

A. Signal Model

As illustrated in Fig. 1, a transmitter equipped with $N_{\rm t}$ transmit antennas intends to send $N_{\rm t}$ independent data symbols to a receiver equipped with $N_{\rm r}$ receive antennas, where $N_{\rm r} \geq N_{\rm t}$. Let $\mathbf{x}[n] = [x_1[n], x_2[n], \ldots, x_{N_{\rm t}}[n]]^\top \in \mathbb{C}^{N_{\rm t}}$ be

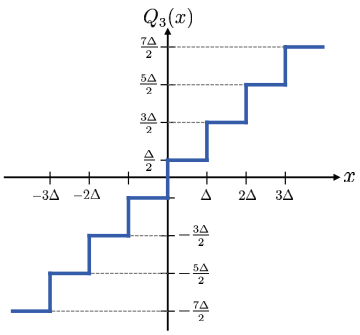

Fig. 2. Illustration of 3-bit uniform scalar quantizer considered in this paper.

the data symbol vector sent by the transmitter at time slot n. The received signal vector $\mathbf{r}[n] \in \mathbb{C}^{N_\mathrm{r}}$ at time slot n before the ADCs is

$$\mathbf{r}[n] = \mathbf{H}\mathbf{x}[n] + \mathbf{z}[n], \tag{1}$$

where $\mathbf{H} \in \mathbb{C}^{N_\mathrm{r} \times N_\mathrm{t}}$ denotes a channel matrix, and $\mathbf{z}[n] = [z_1[n], z_2[n], \ldots, z_{N_\mathrm{r}}[n]]^\top$ is a noise vector in which the element are assumed to be circularly-symmetric complex Gaussian noise with zero mean and variance σ^2, i.e., $z_i[n] \sim \mathcal{CN}(0, \sigma^2)$. Each data symbol $x_i[n]$ satisfies $\mathbb{E}[|x_i[n]|^2] = 1$ and is drawn from a constellation set $\mathcal{X}$ with constellation size $M = |\mathcal{X}|$. For instance, $\mathcal{X} = \{-1, +1\}$ for BPSK modulation. The SNR of the considered system is defined as $\rho = \frac{N_\mathrm{t}}{\sigma^2}$.

We assume a block-fading channel in which the channel remains constant for T time slots. A transmission frame that consists of T time slots is divided into 1) a channel-training phase and 2) a data-transmission phase. The first T_t time slots are allocated for the training phase, and the subsequent T_d time slots are allocated for the data-transmission phase, i.e., $T = T_\mathrm{t} + T_\mathrm{d}$. In this paper, we assume that the transmitter does not have CSIT and, more importantly, that the receiver does not have explicit knowledge of $\mathbf{H}$. Instead, the receiver learns the effective nonlinear channel function by sending a training sequence during the channel-training phase, as will be explained in Section IV-A.

B. ADC Model

Each antenna of the receiver is equipped with an RF chain followed by two low-resolution ADCs that are applied to real and imaginary parts of the received signal, respectively. Each ADC performs element-wise B-bit scalar quantization to the input signal. We adopt B-bit uniform scalar quantizer at the ADCs, defined as

$$Q_B(x) = \begin{cases} r_\mathrm{low} - 0.5\Delta, & x < r_\mathrm{low}, \\ r_\mathrm{low} + \left\lfloor \frac{1}{\Delta}(x - r_\mathrm{low}) \right\rfloor \Delta + 0.5\Delta, & r_\mathrm{low} \le x < r_\mathrm{up}, \\ r_\mathrm{up} + 0.5\Delta, & r_\mathrm{up} \le x, \end{cases} \tag{2}$$

where $r_\mathrm{low} = (-2^{B-1} + 1)\Delta$, $r_\mathrm{up} = (2^{B-1} - 1)\Delta$, and Δ is the step size of the uniform quantizer. The set of all possible outputs of this quantizer is

$$\mathcal{Y} = \left\{(-2^{B-1}+0.5)\Delta, (-2^{B-1}+1.5)\Delta, \ldots, (2^{B-1}-0.5)\Delta\right\}, \tag{3}$$

where $|\mathcal{Y}| = 2^B$. As an example, the 3-bit uniform scalar quantizer considered in this paper is illustrated in Fig. 2. The total ADC process can be described using a function $Q : \mathbb{C}^{N_\mathrm{r}} \to \mathcal{Y}^{2N_\mathrm{r}}$ defined as

$$Q(\mathbf{x}) = [Q_B(x_{\mathrm{R},1}), Q_B(x_{\mathrm{R},2}), \ldots, Q_B(x_{\mathrm{R},2N_\mathrm{R}})]^\top, \tag{4}$$

where $x_{\mathrm{R},i}$ is the ith element of $\mathbf{x}_\mathrm{R}$, and $\mathbf{x}_\mathrm{R} = \left[\mathrm{Re}(\mathbf{x})^\top, \mathrm{Im}(\mathbf{x})^\top\right]^\top$. Using (4), the real-domain received signal vector $\mathbf{y}[n] \in \mathcal{Y}^{2N_\mathrm{r}}$ at time slot n after the ADCs is represented simply as $\mathbf{y}[n] = Q(\mathbf{r}[n])$.

III. Motivation

In this section, we explain the key idea of the proposed blind detection approach by providing a motivating example, then provide some advantages and challenges of the proposed approach.

A. Motivating Example

Consider a real-coefficient MIMO channel with $N_\mathrm{t} = 2$ and $N_\mathrm{r} = 2$, for which the coefficients are given by

$$\mathbf{H} = \begin{bmatrix} 0.5 & 1 \\ 1 & 0 \end{bmatrix}. \tag{5}$$

When BPSK modulation is used at the transmitter, i.e., $\mathcal{X} = \{-1, +1\}$, the transmitter equipped with two transmit antennas is capable of sending four symbol vectors:

$$\mathbf{x}_1 = \begin{bmatrix} 1 \\ 1 \end{bmatrix}, \ \mathbf{x}_2 = \begin{bmatrix} 1 \\ -1 \end{bmatrix}, \ \mathbf{x}_3 = \begin{bmatrix} -1 \\ 1 \end{bmatrix}, \text{ and } \mathbf{x}_4 = \begin{bmatrix} -1 \\ -1 \end{bmatrix}. \tag{6}$$

The set of the possible symbol vectors is denoted as $\mathcal{X}^2 = \{\mathbf{x}_1, \mathbf{x}_2, \mathbf{x}_3, \mathbf{x}_4\}$, and the index set of $\mathcal{X}^2$ is denoted as $\mathcal{K} = \{1, 2, 3, 4\}$. Our strategy for channel-training and data-transmission phases are explained below.

1) **Channel-training phase:** The transmitter uses a training sequence $\mathbf{X}_\mathrm{t} = [\mathbf{x}[1], \mathbf{x}[2], \mathbf{x}[3], \mathbf{x}[4]] = [\mathbf{x}_1, \mathbf{x}_2, \mathbf{x}_3, \mathbf{x}_4]$ to send all possible symbol vectors to the receiver by spanning $T_\mathrm{t} = 4$ time slots. Under the premise that the noise signal is ignored during the training phase, the output signals of the one-bit ADCs with $\Delta = 2$ are:

$$\mathbf{y}[1] = \begin{bmatrix} 1 \\ 1 \end{bmatrix}, \ \mathbf{y}[2] = \begin{bmatrix} -1 \\ 1 \end{bmatrix}, \ \mathbf{y}[3] = \begin{bmatrix} 1 \\ -1 \end{bmatrix}, \text{ and } \mathbf{y}[4] = \begin{bmatrix} -1 \\ -1 \end{bmatrix}. \tag{7}$$

By letting $\mathbf{y}_k = \mathbf{y}[k]$ for $k \in \{1, 2, 3, 4\}$, the set of the above four received signals is denoted by $\mathcal{Y}_\mathrm{t} = \{\mathbf{y}_1, \mathbf{y}_2, \mathbf{y}_3, \mathbf{y}_4\}$. In the training phase, the receiver is assumed to know the training sequence $\mathbf{X}_\mathrm{t} = [\mathbf{x}_1, \mathbf{x}_2, \mathbf{x}_3, \mathbf{x}_4]$. Under this assumption, the receiver generates a set $\mathcal{T} = \{(\mathbf{y}_k, \mathbf{x}_k) | k \in \{1, 2, 3, 4\}\}$ of the four received-signal-and-symbol-vector pairs.

2) **Data-transmission phase:** By using $\mathcal{T}$, the receiver determines a mapping function $f : \mathcal{Y}^{2N_\mathrm{r}} \to \mathcal{K}$ that maps the received signal vector to the index of the symbol vector. Then from the mapping function f, the receiver estimates which symbol vector was transmitted. One possible mapping-function design is to assign the index of the vector in $\mathcal{Y}_\mathrm{t}$ that is

closest to the received signal vector $\mathbf{y}[n]$ for $n \in \{5, 6, \ldots, T\}$. This mapping function is represented as

$$f(\mathbf{y}[n]) = \underset{k\in\{1,2,3,4\}}{\operatorname{argmin}} \|\mathbf{y}[n] - \mathbf{y}_k\|_2 \text{ for } n \in \{5, 6, \ldots, T\}, \tag{8}$$

where $\|\cdot\|_2$ is the Euclidean norm. From (8), the detected symbol vector is obtained as $\hat{\mathbf{x}}[n] = \mathbf{x}_{f(\mathbf{y}[n])}$ for $n \in \{5, 6, \ldots, T\}$. For example, if the transmitter sends $\mathbf{x}_3 = [-1,\ 1]^\top$ at time slot 5, the received signal is $\mathbf{y}[5] = [1, -1]^\top$. From (8), the receiver chooses the index of the transmitted symbol vector as

$$f(\mathbf{y}[5]) = \underset{k\in\{1,2,3,4\}}{\operatorname{argmin}} \|\mathbf{y}[5] - \mathbf{y}_k\|_2 \ = 3. \tag{9}$$

As a result, the receiver correctly estimates the transmitted symbol vector as $\hat{\mathbf{x}}[5] = \mathbf{x}_3$.

B. Connection to Supervised Learning

We can interpret the proposed blind detection framework with the lens of a classification problem in supervised learning. To show this relationship, we first review the key concept of supervised learning in the context of the classification problem. Suppose that an input space $\mathcal{F}$ and a class-label set $\mathcal{S}$ exist such that all feature vectors in $\mathcal{F}$ are associated with one of the class labels in $\mathcal{S}$, according to a fixed but unknown rule (or function). The major goal of supervised learning is to design a classifier (or predictor) $f_{\mathrm{SL}} : \mathcal{F} \to \mathcal{S}$ that can correctly output the class label for every input (feature) vector. Specifically, to design the classifier, supervised learning uses a training set $\mathcal{T}_{\mathrm{SL}} = \{(\mathbf{f}_k, s_k)\,|k \in \mathcal{U},\ \mathcal{U} \subset \{1, \ldots, |\mathcal{F}|\}\}$ where $(\mathbf{f}_k, s_k)$ is the kth training example that informs the known association between $\mathbf{f}_k \in \mathcal{F}$ and $s_k \in \mathcal{S}$, i.e., s_k is the class label of $\mathbf{f}_k$, and $\mathcal{U}$ is the index set of the training examples.

The proposed framework is closely connected to supervised learning. The determination of the mapping function f using the training examples $(\mathbf{y}_k, \mathbf{x}_k)$ for $k \in \{1, 2, 3, 4\}$ is the equivalent to the design of a classifier $f : \mathcal{Y}_{\mathrm{t}} \to \mathcal{K}$ by using the training set $\mathcal{T} = \{(\mathbf{y}_k, \mathbf{x}_k)|k \in \{1, 2, 3, 4\}\}$. Here, the index of the symbol vector and the received signal correspond to a class label and a feature vector, respectively. In this context, the classifier f serves as the decoding function, because the index of the symbol vector for the received signal $\mathbf{y}[n]$, $n \geq 5$, is detected as $k^\star[n] = f(\mathbf{y}[n])$. As a result, determining a good decoding function that accurately detects the symbol vector is equivalent to designing a good classifier that correctly assigns the class label.

C. Why is Blind Detection Possible and Useful?

As shown in the motivating example, the proposed framework does not use explicit knowledge of $\mathbf{H}$. Instead, the receiver detects the input data symbols by exploiting the mapping function f, which characterizes the nonlinear input-output relation of the system including both $\mathbf{H}$ and the quantizer. This allows us to perform blind detection by learning the mapping function f at the receiver without knowledge of explicit CSIR. This blind detection concept differs from the previous blind detection approach that uses joint channel-and-data estimation method [12]. The proposed blind detection is particularly useful in MIMO systems with low-resolution ADCs, where accuracy of CSIR obtained by conventional channel estimation techniques is insufficient to support coherent detection. Therefore, the proposed blind detection framework is less subject to the nonlinear distortion effects by the ADCs and to possible hardware impairments (e.g. I/Q imbalance), because the proposed framework learns the nonlinear function itself.

D. Challenges in Learning f

At a glance, the proposed blind detection framework using the supervised-learning concept seems simple, but in practice, application of this framework for a general MIMO communication system entails two major challenges:

- **Channel ambiguity:** For some realizations of channel matrix $\mathbf{H}$, the received signals from two different symbol vectors can be identical even without noise, i.e., $Q(\mathbf{H}\mathbf{x}_i) = Q(\mathbf{H}\mathbf{x}_j)$ for $i \neq j$. Because of this identity, these two symbol vectors cannot be distinguished using the corresponding received vectors when employing the supervised-learning framework.
- **Noise ambiguity:** Classification ambiguity can also be caused by noise. Specifically, during the training phase, two different symbol vectors can be the same as a result of the effect of noise i.e., $Q(\mathbf{H}\mathbf{x}_i + \mathbf{z}[n]) = Q(\mathbf{H}\mathbf{x}_j + \mathbf{z}[m])$ for $n, m \in \{1, \ldots, T_{\mathrm{t}}\}$ when $Q(\mathbf{H}\mathbf{x}_i) \neq Q(\mathbf{H}\mathbf{x}_j)$.

Either type of classification ambiguity causes failure to determine a correct mapping function f, and therefore results in a detection error during the subsequent data-transmission phase. In particular, the classification ambiguity caused by the channel can significantly degrade the SER of the system, so this ambiguity problem should be analyzed. In the sequel, to understand how the channel ambiguity problem affect the SER, we present analytical characterizations of practical MIMO systems with one-bit ADCs.

IV. Blind MIMO Detection Techniques

In this section, inspired by the classification approach in supervised learning, we propose blind detection techniques for MIMO systems with low-resolution ADCs. We first introduce two channel-training methods to learn a decoding function, then present three symbol-detection methods.

A. Channel-Training Methods

The principal goal of the channel training is to learn f by using T_{t} input-output pairs for a given channel matrix $\mathbf{H}$. Unfortunately, unlike in the motivating example, this channel training is not straightforward because noise makes a received signal to be a random vector even when the transmitter sends the same symbol vector through a fixed channel. Therefore, to resolve this problem, we develop two different channel-training methods.

1) Full Channel-Training Method: The key idea of the full channel-training method is to repeatedly send each symbol vector so that the receiver observes the multiple received signals for each symbol vector. These multiple observations allow the receiver to obtain an empirical conditional distribution of the received signals for each symbol vector. The detailed procedures of the full channel-training method is given below.

When the transmitter equipped with N_{t} transmit antennas sends a data symbol vector using a constellation set $\mathcal{X}$, the set of all possible symbol vectors is denoted as $\mathcal{X}^{N_{\mathrm{t}}}$, and the number of possible symbol vectors is given by $K = M^{N_{\mathrm{t}}}$. Let $\mathbf{x}_k$ be the kth possible symbol vector and L be the number of repetitions of each input vector during training phase. Then the training-sequence matrix for the full channel-training method is given by

$$\begin{aligned}\mathbf{X}_{\mathrm{t}} &= [\mathbf{x}[1],\ \mathbf{x}[2], \ldots, \mathbf{x}[T_{\mathrm{t}}]] \\ &= \left[\underbrace{\mathbf{x}_1, \ldots, \mathbf{x}_1}_{L \text{ repetition}}, \mathbf{x}_2, \ldots, \mathbf{x}_2, \ldots\ldots, \mathbf{x}_K, \ldots, \mathbf{x}_K\right]. \quad (10)\end{aligned}$$

This training method requires a total of KL time slots for the period of training, i.e., $T_{\mathrm{t}} = KL$. We assume that the receiver has perfect knowledge of both $\mathcal{X}^{N_{\mathrm{t}}}$ and L or equivalently $\mathbf{X}_{\mathrm{t}}$. Under this premise, the receiver observes the set of the signal vectors associated with the kth symbol vector, denoted by $\mathcal{Y}_{\mathrm{t},k} = \{\mathbf{y}[n] | n \in \{(k-1)L+1, \ldots, kL\}\}$. Therefore, the set of received signals learned from the channel training is $\mathcal{Y}_{\mathrm{t}} = \cup_{k=1}^{K} \mathcal{Y}_{\mathrm{t},k} \subset \mathcal{Y}^{2N_{\mathrm{r}}}$.

In detection theory, a conditional probability function is a sufficient statistic to perform ML detection. Motivated by this, using $\mathcal{Y}_{\mathrm{t},k}$, the receiver creates an empirical conditional PMF for each symbol vector $\mathbf{x}_k$ as follows:

$$\hat{p}(\tilde{\mathbf{y}}|\mathbf{x}_k) = \frac{1}{L}\sum_{t=1}^{L} \mathbf{1}\left(\tilde{\mathbf{y}} = \mathbf{y}[(k-1)L+t]\right), \quad (11)$$

where $k \in \{1, 2, \ldots, K\}$ and $\mathbf{1}(A)$ is an indicator function that equals 1 if an event A is true and 0 otherwise. We will present how to use this empirical conditional PMF for the data detection in the next subsection.

2) Efficient Channel-Training Method: In the full channel-training method, the length of the training sequence is given by $T_{\mathrm{t}} = KL$. Somewhat surprisingly, this length can be reduced by the half if the system satisfies two conditions:

- The quantization function of the ADCs is symmetric with respect to the origin, i.e., $Q(-\mathbf{r}) = -Q(\mathbf{r})$.
- The constellation map is symmetric with respect to the origin, i.e., $-x \in \mathcal{X}$ for all $x \in \mathcal{X}$.

To get an insight for this reduction, we set the indexes of the symbol vectors to satisfy $\mathbf{x}_{K-i+1} = -\mathbf{x}_i$ for all i. Note that this is possible only when the second condition is satisfied. Then we have

$$\begin{aligned}\mathbf{y}[(i-1)L+t] &= Q\left(\mathbf{H}\mathbf{x}_i + \mathbf{z}[n]\right) \\ &\overset{\mathrm{d}}{=} Q\left(\mathbf{H}\mathbf{x}_i - \mathbf{z}[n]\right) \\ &= -Q\left(\mathbf{H}\mathbf{x}_{K-i+1} + \mathbf{z}[n]\right) \\ &= -\mathbf{y}[(K-i)L+t], \quad (12)\end{aligned}$$

for $i \in \left\{1, 2, \ldots, \frac{K}{2}\right\}$ and $t \in \{1, 2, \ldots, L\}$, where $\overset{\mathrm{d}}{=}$ denotes equality in distribution. Note that the third equality in (12) holds only when the first condition is satisfied.

Motivated by the equations in (12), we propose an *efficient* channel-training method that reduces the training duration of the full channel-training method by the half. The training-sequence matrix for this efficient channel-training method is given by

$$\begin{aligned}\mathbf{X}'_{\mathrm{t}} &= [\mathbf{x}[1],\ \mathbf{x}[2], \ldots, \mathbf{x}[T_{\mathrm{t}}]] \\ &= \left[\underbrace{\mathbf{x}_1, \ldots, \mathbf{x}_1}_{L \text{ repetition}}, \mathbf{x}_2, \ldots, \mathbf{x}_2, \ldots\ldots, \mathbf{x}_{\frac{K}{2}}, \ldots, \mathbf{x}_{\frac{K}{2}}\right], \quad (13)\end{aligned}$$

where the indexes of the symbol vectors are assigned to satisfy $\mathbf{x}_{K-i+1} = -\mathbf{x}_i$ for all i. The required number of time slots to send the above training sequence is $T_{\mathrm{t}} = \frac{KL}{2}$. Then the receiver creates the empirical conditional PMFs for all symbol vectors according to

$$\begin{aligned}&\hat{p}(\tilde{\mathbf{y}}|\mathbf{x}_k) \\ &= \begin{cases} \frac{1}{L}\sum_{t=1}^{L} \mathbf{1}\left(\tilde{\mathbf{y}} = \mathbf{y}[(k-1)L+t]\right), & k \in \left\{1, \ldots, \frac{K}{2}\right\}, \\ \frac{1}{L}\sum_{t=1}^{L} \mathbf{1}\left(\tilde{\mathbf{y}} = -\mathbf{y}[(K-k)L+t]\right), & k \in \left\{\frac{K}{2}+1, \ldots, K\right\}, \end{cases} \quad (14)\end{aligned}$$

Therefore, the receiver is possible to generate the empirical conditional PMFs for all symbol vectors without sending the training sequence for the symbol vectors $\mathbf{x}_{\frac{K}{2}+1}, \ldots, \mathbf{x}_K$. Fortunately, this strategy is applied to the most practical communication systems as the stair-type quantizer and both quadrature amplitude modulation (QAM) and PSK modulation satisfy the two conditions. This efficient channel-training method is extremely useful, especially when L is large.

B. Symbol-Detection Methods

We describe three detection methods that exploit the empirical conditional PMF obtained during the training phase.

1) Empirical-Maximum-Likelihood Detection (eMLD): The key idea of eMLD is to select the index of the input symbol vector that maximizes the empirical conditional PMF, namely,

$$k^{\star}[n] = \underset{k}{\operatorname{argmax}}\, \hat{p}(\mathbf{y}[n]|\mathbf{x}_k). \quad (15)$$

When the number of repetitions approaches infinity, this detection strategy is the same as the optimal ML detection method, because the empirical distribution converges to the corresponding true distribution by the law of large numbers. When L is insufficient, however, there is a non-zero probability that $\mathbf{y}[n] \notin \mathcal{Y}_{\mathrm{t}} = \cup_{k=1}^{K} \mathcal{Y}_{\mathrm{t},k}$. In this case, the detection method in (15) fails to detect a correct symbol vector because $\hat{p}(\mathbf{y}[n]|\mathbf{x}_k) = 0$ for all k. To resolve this problem, we find a set of vectors that are closest to $\mathbf{y}[n]$ among the received signal vectors in $\mathcal{Y}_{\mathrm{t}}$, and then use these vectors to select the optimal index k, as illustrated in Fig. 3(a). Let $\mathcal{N}(\mathbf{y}[n])$ be the set of the closest vectors to $\mathbf{y}[n]$ among the vectors in $\mathcal{Y}_{\mathrm{t}}$ with respect to the Euclidean distance, i.e.,

$$\mathcal{N}(\mathbf{y}[n]) = \left\{\mathbf{y} \;\middle|\; \|\mathbf{y}[n] - \mathbf{y}\|_2 = R_{\min}[n],\ \mathbf{y} \in \mathcal{Y}_{\mathrm{t}}\right\}, \quad (16)$$

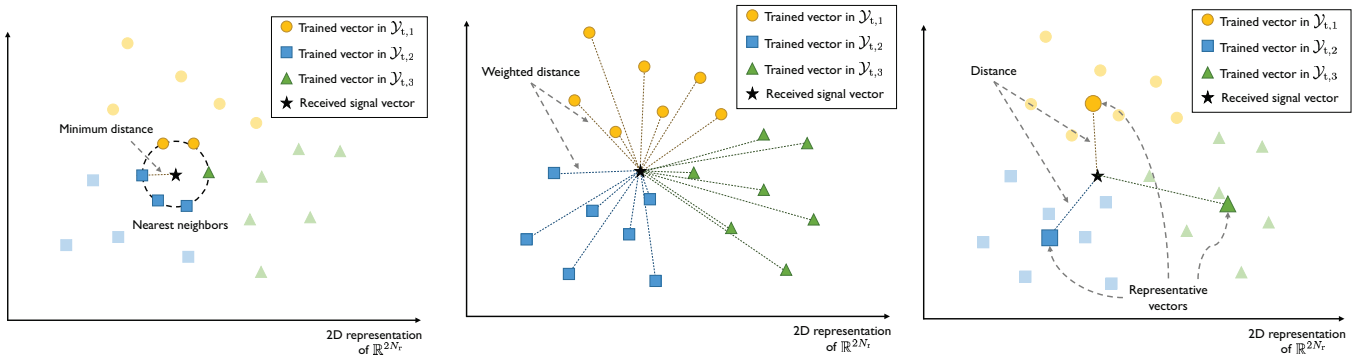

(a) Empirical-maximum-likelihood detection (b) Minimum-mean-distance detection (c) Minimum-center-distance detection

Fig. 3. Illustration for key concepts of three proposed detection methods when $K = 3$.

where $R_{\min}[n] = \min_{\mathbf{y}\in\mathcal{Y}_t} \|\mathbf{y}[n] - \mathbf{y}\|_2$. From (16), the proposed eMLD method, $f_{\text{eMLD}} : \mathcal{Y}^{2N_r} \to \mathcal{K} = \{1, 2, \ldots, K\}$, is given by

$$f_{\text{eMLD}}(\mathbf{y}[n]) = \underset{k}{\text{argmax}} \sum_{\mathbf{y}\in\mathcal{N}(\mathbf{y}[n])} \hat{p}(\mathbf{y}|\mathbf{x}_k). \tag{17}$$

Connection to a K-nearest neighbors (KNN) classifier: The proposed eMLD method resembles with a KNN classifier, which is widely used to solve the classification problem in supervised learning. The key idea of the KNN classifier is that when an unlabeled vector is observed, it finds the K-nearest neighbors to the observed vector, and assigns a label to the vector by using the majority voting of neighbors' labels. As explained, eMLD finds the neighbor set $\mathcal{N}(\mathbf{y}[n])$, and then assigns the index $f_{\text{eMLD}}(\mathbf{y}[n])$ as the most probably index for the vectors in $\mathcal{N}(\mathbf{y}[n])$. Therefore, the eMLD method is almost identical to the KNN classifier in the sense that they simply compare the number of neighbors' labels. The only difference is that eMLD uses the neighbor set of elements that are equidistant from the received vector.

2) Minimum-Mean-Distance Detection (MMD): Unfortunately, eMLD partially uses the empirical conditional PMFs, because it finds the index that maximizes the sum of the empirical PMFs of the nearest neighbors only. This partial exploitation of the empirical PMFs may result in a high symbol-detection error when L is insufficient. Therefore, to fully exploit the empirical PMFs, we present an alternative blind detection method, which is called MMD.

The key idea of MMD is to compare the mean of the distances from a received signal using the empirical PMF. As illustrated in Fig. 3(b), the proposed MMD method, $f_{\text{MMD}} : \mathcal{Y}^{2N_r} \to \mathcal{K} = \{1, 2, \ldots, K\}$, selects the index of the symbol vector that yields the conditional minimum mean distance, i.e.,

$$\begin{aligned} f_{\text{MMD}}(\mathbf{y}[n]) &= \underset{k}{\text{argmin}}\, \mathbb{E}\left[\|\mathbf{y}[n] - \mathbf{y}\|_2 \,|\mathbf{x} = \mathbf{x}_k\right] \\ &\triangleq \underset{k}{\text{argmin}} \sum_{\mathbf{y}\in\mathcal{Y}_t} \|\mathbf{y}[n] - \mathbf{y}\|_2 \,\hat{p}\left(\mathbf{y}|\mathbf{x}_k\right). \end{aligned} \tag{18}$$

As can be seen in (18), MMD differs from eMLD. On the one hand, MMD finds the index that *minimizes* the *weighted* sum of the empirical PMFs, where the weights are the distance between the received vector and the trained vector, $\|\mathbf{y}[n] - \mathbf{y}\|_2$ for all $\mathbf{y} \in \mathcal{Y}_t$. On the other hand, eMLD finds the index that *maximizes* the *non-weighted* sum of the empirical PMFs. Although the optimality of MMD is not guaranteed, it may perform better than eMLD when L is insufficient, because MMD additionally uses reliability information captured by the distance between the received signal and the trained signal.

3) Minimum-Center-Distance Detection (MCD): One drawback of eMLD and MMD is that they entail high computational complexity. In both methods, the receiver requires to compute all distances among the received signal and the vectors in $\mathcal{Y}_t$. Particularly, when the size of $\mathcal{Y}_t$ is large (e.g., $L \gg 1$), the complexities of these two methods may not be acceptable for use in practical systems. Therefore, to reduce the detection complexity, we present a simple blind detection method, called MCD.

The key idea of MCD is to create a set of K representative vectors at the receiver for decoding as depicted in Fig. 3(c). Specifically, during the training phase, the receiver has observed L output vectors $\mathcal{Y}_{t,k} = \{\mathbf{y}[(k-1)L+1], \ldots, \mathbf{y}[kL]\}$ for each symbol vector $\mathbf{x}_k$. We create a representative output vector for the kth input vector $\mathbf{x}_k$ by computing the empirical conditional expectation, i.e.,

$$\begin{aligned} \mathbb{E}[\mathbf{y}|\mathbf{x}_k] &\triangleq \sum_{\mathbf{y}\in\mathcal{Y}_{t,k}} \mathbf{y}\hat{p}(\mathbf{y}|\mathbf{x}_k) \\ &= \frac{1}{L}\sum_{t=1}^{L} \mathbf{y}[(k-1)L + t]. \end{aligned} \tag{19}$$

Notice that $\mathbb{E}[\mathbf{y}|\mathbf{x}_k]$ is not necessarily an element of $\mathcal{Y}^{2N_r}$. Utilizing $\mathbb{E}[\mathbf{y}|\mathbf{x}_k]$ for $k \in \{1, 2, \ldots, K\}$, the proposed MCD method, $f_{\text{MCD}} : \mathcal{Y}^{2N_r} \to \mathcal{K}$, finds the index that minimizes the distance between $\mathbf{y}[n]$ and $\mathbb{E}[\mathbf{y}|\mathbf{x}_k]$ as follows:

$$f_{\text{MCD}}(\mathbf{y}[n]) = \underset{k}{\text{argmin}} \left\|\mathbf{y}[n] - \mathbb{E}[\mathbf{y}|\mathbf{x}_k]\right\|_2. \tag{20}$$

Connection to a nearest-centroid classifier (NCC): We explain the proposed MCD method with the lens of NCC. NCC is a simple supervised-learning method that assigns the class label of a unlabeled observed vector by using the centroid vectors that represent their classes. The principle of

MCD is very close to this learning method, because MCD determines the index of the detected symbol vector as the index with the minimum distance from the conditional mean vector of the trained signals, each of which is associated with an input symbol vector. Therefore, MCD can be interpreted as the application of NCC to the detection problem in wireless communications.

V. Analysis for MIMO systems With One-Bit ADCs

This section provides the analytical characterizations of the detection-error performance for MIMO systems with one-bit ADCs when BPSK modulation is used. Although the analysis focuses on the simple case, it is sufficient to reveal how the channel and noise ambiguity affect the detection-error performance for the MIMO systems with low-resolution ADCs.

A. Symbol-Vector-Error Probability

We first present the analytical expression for the upper bound of the symbol-vector-error probability when the MCD method is used.

Theorem 1. *Suppose the number of repetitions of each symbol vector for the training is sufficiently large. When MCD is applied, the upper bound of the symbol-vector-error probability* $P_{\mathrm{e}}^{\mathrm{vec}}$ *is*

$$P_{\mathrm{e}}^{\mathrm{vec}} \leq \sum_{j=D}^{2N_{\mathrm{r}}} \binom{2N_{\mathrm{r}}}{j} \exp\left(-\frac{D\rho g_{\min}^2}{N_{\mathrm{t}}}\right), \tag{21}$$

where $D = \left\lfloor \frac{d_{\min}+1}{2} \right\rfloor$, $d_{\min} = \min_{i\neq j} \left\|Q(\mathbf{H}\mathbf{x}_i) - Q(\mathbf{H}\mathbf{x}_j)\right\|_0$, $g_{\min} = \min_{(k,l)} |g_{k,l}|$, $g_{k,l}$ *is the* l*th element of* $\mathbf{g}_k$*, and* $\mathbf{g}_k = \left[\mathrm{Re}\left(\mathbf{H}\mathbf{x}_k\right)^\top,\ \mathrm{Im}\left(\mathbf{H}\mathbf{x}_k\right)^\top\right]^\top$.

Proof: In this proof, we omit the index n of time slot for ease of exposition. Suppose that the transmitter sends a BPSK signal vector $\mathbf{x} \in \{-1,+1\}^{N_{\mathrm{t}}}$ and the receiver is equipped with one-bit ADCs with $\Delta = 2$. When MCD is applied, the receiver detects the symbol vector as $\hat{\mathbf{x}} = \mathbf{x}_{k^\star}$, where $k^\star = f_{\mathrm{MCD}}(\mathbf{y})$, and $\mathbf{y} = Q(\mathbf{H}\mathbf{x}+\mathbf{n}) \in \{-1,+1\}^{2N_{\mathrm{r}}}$. Let $P_{\mathrm{e},k}^{\mathrm{vec}} = \mathbb{P}\left(\hat{\mathbf{x}} \neq \mathbf{x}_k | \mathbf{x} = \mathbf{x}_k\right)$ be the pair-wise error probability that the detected symbol vector is different from $\mathbf{x}_k$ when the transmitter sends $\mathbf{x}_k$. Then the symbol-vector-error probability is defined as

$$P_{\mathrm{e}}^{\mathrm{vec}} = \sum_{k=1}^{2^{N_{\mathrm{t}}}} \mathbb{P}\left(\hat{\mathbf{x}} \neq \mathbf{x}_k, \mathbf{x} = \mathbf{x}_k\right) = \frac{1}{2^{N_{\mathrm{t}}}} \sum_{k=1}^{2^{N_{\mathrm{t}}}} P_{\mathrm{e},k}^{\mathrm{vec}}. \tag{22}$$

If the number of repetitions for the training is sufficiently large, the MCD method obtains the K representative vectors as

$$\mathbb{E}[\mathbf{y}|\mathbf{x}_k] = \lim_{L\to\infty} \frac{1}{L} \sum_{t=1}^{L} \mathbf{y}[(k-1)L+t] = Q(\mathbf{H}\mathbf{x}_k), \tag{23}$$

where $k \in \mathcal{K}$. Then the detection rule of the MCD method in (20) with the one-bit ADCs is rewritten as

$$\begin{aligned} k^\star[n] &= \operatorname*{argmin}_k \left\|\mathbf{y} - Q(\mathbf{H}\mathbf{x}_k)\right\|_2 &(24)\\ &= \operatorname*{argmin}_k \left\|\mathbf{y} - Q(\mathbf{H}\mathbf{x}_k)\right\|_0, &(25)\end{aligned}$$

where the equality of (25) holds only for the one-bit-ADC case, and $\|\mathbf{a}\|_0$ is the zero norm that denotes the number of nonzero elements in a vector $\mathbf{a}$.

From (25), $P_{\mathrm{e},i}^{\mathrm{vec}}$ of the MCD method is upper bounded as

$$P_{\mathrm{e},k}^{\mathrm{vec}} \leq \mathbb{P}\left(\left\|\mathbf{y}-Q(\mathbf{H}\mathbf{x}_k)\right\|_0 \geq \min_{j\neq k} \left\|\mathbf{y}-Q(\mathbf{H}\mathbf{x}_j)\right\|_0 \middle| \mathbf{x} = \mathbf{x}_k\right). \tag{26}$$

For further analysis, we define a set $\mathcal{C} = \{Q(\mathbf{H}\mathbf{x}_1), Q(\mathbf{H}\mathbf{x}_2), \ldots, Q(\mathbf{H}\mathbf{x}_K)\}$. We interpret this set as an error-correcting code; each element $Q(\mathbf{H}\mathbf{x}_k) = \mathbb{E}[\mathbf{y}|\mathbf{x}_k]$ can be treated as a codeword vector of $\mathcal{C}$. For any code, one can define the minimum distance of the code as

$$d_{\min}(\mathbf{H}, Q(\cdot)) = \min_{i\neq j} \left\|Q(\mathbf{H}\mathbf{x}_i) - Q(\mathbf{H}\mathbf{x}_j)\right\|_0. \tag{27}$$

The proposed detection method causes an error when $\mathbf{x}_k$ was sent, provided that $\left\|\mathbf{y} - Q(\mathbf{H}\mathbf{x}_k)\right\|_0 \geq D$, where $D = \left\lfloor \frac{d_{\min}+1}{2} \right\rfloor$. Thus, we obtain an upper bound as

$$\begin{aligned} P_{\mathrm{e},k}^{\mathrm{vec}} &\leq \mathbb{P}\left(\left\|\mathbf{y} - Q(\mathbf{H}\mathbf{x}_k)\right\|_0 \geq D \middle| \mathbf{x} = \mathbf{x}_k\right)\\ &= \mathbb{P}\left(\left\|Q(\mathbf{H}\mathbf{x}_k + \mathbf{z}) - Q(\mathbf{H}\mathbf{x}_k)\right\|_0 \geq D\right)\\ &= \mathbb{P}\left(\sum_{l=1}^{2N_{\mathrm{r}}} \mathrm{I}\left(Q_1(g_{k,l} + z_{\mathrm{R},l}) \neq Q_1(g_{k,l})\right) \geq D\right)\\ &= \mathbb{P}\left(\sum_{l=1}^{2N_{\mathrm{r}}} \mathrm{I}\left(\mathrm{sign}(g_{k,l} + z_{\mathrm{R},l}) \neq \mathrm{sign}(g_{k,l})\right) \geq D\right), \end{aligned} \tag{28}$$

where $\mathrm{sign}(\cdot)$ is the signum function, $g_{k,l}$ is the lth element of $\mathbf{g}_k$, $z_{\mathrm{R},l}$ is the lth element of $\mathbf{z}_{\mathrm{R}}$,

$$\mathbf{g}_k = \begin{bmatrix} \mathrm{Re}\left(\mathbf{H}\mathbf{x}_k\right) \\ \mathrm{Im}\left(\mathbf{H}\mathbf{x}_k\right) \end{bmatrix}, \text{ and } \mathbf{z}_{\mathrm{R}} = \begin{bmatrix} \mathrm{Re}(\mathbf{z}) \\ \mathrm{Im}(\mathbf{z}) \end{bmatrix}. \tag{29}$$

Because $z_{\mathrm{R},l}$ is independent and identically distributed (IID) as $\mathcal{N}(0, \frac{\sigma^2}{2})$ for all l, the probability that the sign of $g_{k,l}$ is flipped due to noise depends only on the magnitude of $g_{k,l}$, where the probability increases as the magnitude of $g_{k,l}$ decreases. Using this fact, we obtain the following inequality:

$$\begin{aligned} &\mathbb{P}\left(\sum_{l=1}^{2N_{\mathrm{r}}} \mathrm{I}\left(\mathrm{sign}(g_{k,l} + z_{\mathrm{R},l}) \neq \mathrm{sign}(g_{k,l})\right) \geq D\right)\\ &\leq \sum_{j=D}^{2N_{\mathrm{r}}} \binom{2N_{\mathrm{r}}}{j} \prod_{l=l_{k,1}^\star}^{l_{k,D}^\star} \mathbb{P}\left(\mathrm{sign}(g_{k,l} + z_{\mathrm{R},l}) \neq \mathrm{sign}(g_{k,l})\right)\\ &= \sum_{j=D}^{2N_{\mathrm{r}}} \binom{2N_{\mathrm{r}}}{j} \prod_{l=l_{k,1}^\star}^{l_{k,D}^\star} \left\{1 - \Phi\left(\sqrt{\frac{2\rho|g_{k,l}|^2}{N_{\mathrm{t}}}}\right)\right\}, \end{aligned} \tag{30}$$

where $l_{k,i}^\star$ is the index of the element of $\mathbf{g}_k$ that has the ith-minimum absolute value, and $\Phi(\cdot)$ is the cumulative distribu-

tion of the standard normal random variable. Aggregating the results in (22), (28), and (30) yields

$$\begin{aligned} P_{\mathrm{e}}^{\mathrm{vec}} &\leq \frac{1}{2^{N_{\mathrm{t}}}} \sum_{j=D}^{2N_{\mathrm{r}}} \binom{2N_{\mathrm{r}}}{j} \sum_{k=1}^{2^{N_{\mathrm{t}}}} \prod_{l=l_{k,1}^{\star}}^{l_{k,D}^{\star}} \left\{ 1 - \Phi\left(\sqrt{\frac{2\rho |g_{k,l}|^2}{N_{\mathrm{t}}}} \right) \right\} \\ &\leq \sum_{j=D}^{2N_{\mathrm{r}}} \binom{2N_{\mathrm{r}}}{j} \left\{ 1 - \Phi\left(\sqrt{\frac{2\rho g_{\min}^2}{N_{\mathrm{t}}}} \right) \right\}^{D} \\ &\leq \sum_{j=D}^{2N_{\mathrm{r}}} \binom{2N_{\mathrm{r}}}{j} \exp\left(-\frac{D\rho g_{\min}^2}{N_{\mathrm{t}}} \right), \end{aligned} \tag{31}$$

where $g_{\min} = \min_{(k,l)} |g_{k,l}|$. This completes the proof. ■

Proposition 1 demonstrates that the upper bound of the symbol-error probability decreases exponentially with SNR, ρ, the minimum channel gain, $g_{\min}^2$, the minimum distance, $D = \left\lfloor \frac{d_{\min}+1}{2} \right\rfloor$, and the inverse of N_{t}. The most interesting parameter here is $d_{\min}$. Because $d_{\min}$ is determined by the channel matrix $\mathbf{H}$ and the quantization function $Q(\cdot)$, it significantly affects the symbol-error probability. In particular, in a certain channel realization $\mathbf{H}$, the received signals from two different symbol vectors $\mathbf{x}_i$ and $\mathbf{x}_j$ cannot be distinguished due to the channel ambiguity, i.e., $Q(\mathbf{H}\mathbf{x}_i) = Q(\mathbf{H}\mathbf{x}_j)$ for $i \neq j$. In this case, the SER increases significantly, which agrees with our intuition.

To reduce the SER, it is important to design the communication system with large enough minimum distance of the code $\mathcal{C} = \{Q(\mathbf{H}\mathbf{x}_1), Q(\mathbf{H}\mathbf{x}_2), \ldots, Q(\mathbf{H}\mathbf{x}_K)\}$. One simple way to enlarge the minimum distance is to increase the number of receive antennas N_{r}. For example, if $N_{\mathrm{t}} = 2$, we have four possible input vectors $\{\mathbf{x}_1, \mathbf{x}_2, \mathbf{x}_3, \mathbf{x}_4\} \in \{-1, +1\}^2$ and a code $\mathcal{C} = \{Q(\mathbf{H}\mathbf{x}_1), Q(\mathbf{H}\mathbf{x}_2), Q(\mathbf{H}\mathbf{x}_3), Q(\mathbf{H}\mathbf{x}_4)\} \in \{-1, +1\}^{2N_{\mathrm{r}}}$ for the communications. Clearly, the minimum distance $d_{\min}$ increases with N_{r}, because each codeword can be mapped into a higher-dimensional space. This characteristic can be interpreted as a *receive diversity gain* in the MIMO system with one-bit ADCs.

B. Distribution of $d_{\min}$ for Rayleigh-Fading Channel

We have shown that the detection-error performance of the MIMO systems with the one-bit ADCs depends on $D = \left\lfloor \frac{d_{\min}+1}{2} \right\rfloor$ for a given channel realization. To provide a more clear understanding for the error performance under a random channel realization, we derive the distribution of $d_{\min}$ by assuming Rayleigh-fading channels.

Theorem 2. *For Rayleigh-fading channels, the approximate complementary cumulative distribution function (CCDF) of $d_{\min} = \min_{i \neq j} \|Q(\mathbf{H}\mathbf{x}_i) - Q(\mathbf{H}\mathbf{x}_j)\|_0$ is*

$$\mathbb{P}\left(d_{\min} \geq n\right) \approx \prod_{1 \leq i < j \leq 2^{N_{\mathrm{t}}}-1} \sum_{k=n}^{2N_{\mathrm{r}}-n} \binom{2N_{\mathrm{r}}}{k} \left(1 - p_{\mathrm{eq},\delta_{i,j}}\right)^k p_{\mathrm{eq},\delta_{i,j}}^{2N_{\mathrm{r}}-k}. \tag{32}$$

where $\delta_{i,j} = \|\mathbf{x}_i - \mathbf{x}_j\|_0$, and $p_{\mathrm{eq},\delta} = \frac{2}{\pi} \arctan\left(\sqrt{\frac{N_{\mathrm{t}}-\delta}{\delta}} \right)$.

Proof: When the BPSK modulation is used for the transmission, for any $\mathbf{x} \in \mathcal{X}^{N_{\mathrm{t}}}$, $-\mathbf{x}$ is also one of the possible symbol vectors. Therefore, we can set the indexes of the symbol vectors to satisfy that $\mathbf{x}_{2^{N_{\mathrm{t}}}-k+1} = -\mathbf{x}_k$ for $k \in \{1, \ldots, 2^{N_{\mathrm{t}}-1}\}$. This process yields

$$\begin{aligned} \mathbb{P}\left(d_{\min} \geq n\right) &= \mathbb{P}\left(\bigcap_{1 \leq i < j \leq 2^{N_{\mathrm{t}}}} \{\|Q(\mathbf{H}\mathbf{x}_i) - Q(\mathbf{H}\mathbf{x}_j)\|_0 \geq n\} \right) \\ &= \mathbb{P}\Bigg(\bigcap_{1 \leq i < j \leq 2^{N_{\mathrm{t}}-1}} \Big[\min\Big\{ \|Q(\mathbf{H}\mathbf{x}_i) - Q(\mathbf{H}\mathbf{x}_j)\|_0, \\ &\qquad \|Q(\mathbf{H}\mathbf{x}_i) - Q(-\mathbf{H}\mathbf{x}_j)\|_0 \Big\} \geq n \Big] \Bigg). \end{aligned} \tag{33}$$

When the receiver is equipped with the one-bit ADCs defined as in (2) and (4), the following equality holds:

$$\|Q(\mathbf{H}\mathbf{x}_i) - Q(\mathbf{H}\mathbf{x}_j)\|_0 + \|Q(\mathbf{H}\mathbf{x}_i) + Q(\mathbf{H}\mathbf{x}_j)\|_0 = 2N_{\mathrm{r}}. \tag{34}$$

Applying (34) to (33) with $Q(-\mathbf{H}\mathbf{x}_j) = -Q(\mathbf{H}\mathbf{x}_j)$ yields

$$\begin{aligned} &\mathbb{P}\left(d_{\min} \geq n\right) \\ &= \mathbb{P}\left(\bigcap_{1 \leq i < j \leq 2^{N_{\mathrm{t}}-1}} \{n \leq \|Q(\mathbf{H}\mathbf{x}_i) - Q(\mathbf{H}\mathbf{x}_j)\|_0 \leq 2N_{\mathrm{r}} - n\} \right). \end{aligned} \tag{35}$$

Notice that when $n > N_{\mathrm{r}}$, the RHS of (35) becomes 0, so $\mathbb{P}\left(d_{\min} \geq N_{\mathrm{r}} + 1\right) = 0$. Unfortunately, exact calculation of the RHS of (35) is difficult due to the complicated correlation among $Q(\mathbf{H}\mathbf{x}_i)$ for all i. Instead, we approximate the RHS of (35) by ignoring the correlation among $Q(\mathbf{H}\mathbf{x}_i)$ as follows:

$$\begin{aligned} &\mathbb{P}\left(d_{\min} \geq n\right) \\ &\approx \prod_{1 \leq i < j \leq 2^{N_{\mathrm{t}}-1}} \mathbb{P}\left(n \leq \|Q(\mathbf{H}\mathbf{x}_i) - Q(\mathbf{H}\mathbf{x}_j)\|_0 \leq 2N_{\mathrm{r}} - n\right). \end{aligned} \tag{36}$$

The probability of each pair event in (36) is calculated as

$$\begin{aligned} &\mathbb{P}\left(n \leq \|Q(\mathbf{H}\mathbf{x}_i) - Q(\mathbf{H}\mathbf{x}_j)\|_0 \leq 2N_{\mathrm{r}} - n\right) \\ &= \sum_{k=n}^{2N_{\mathrm{r}}-n} \mathbb{P}\left(\|Q(\mathbf{H}\mathbf{x}_i) - Q(\mathbf{H}\mathbf{x}_j)\|_0 = k\right) \\ &= \sum_{k=n}^{2N_{\mathrm{r}}-n} \mathbb{P}\left(\sum_{l=1}^{2N\mathrm{r}} \mathbf{1}\left(\mathrm{sign}(g_{i,l}) \neq \mathrm{sign}(g_{j,l})\right) = k \right), \end{aligned} \tag{37}$$

where the equality of (37) follows from (2). For Rayleigh-fading channels, each channel element is drawn from an IID circularly-symmetric complex Gaussian random variable with zero mean and unit variance. Therefore, for each symbol vector

$\mathbf{x}_i \in \{-1,+1\}^{N_\mathrm{t}}$, all elements of $\mathbf{g}_i$ defined in (29) are IID as $\mathcal{N}\left(0, \frac{N_\mathrm{t}}{2}\right)$. Using this fact, the RHS of (37) is rewritten as

$$\begin{aligned}&\mathbb{P}\left(n \le \|Q(\mathbf{H}\mathbf{x}_i) - Q(\mathbf{H}\mathbf{x}_j)\|_0 \le 2N_\mathrm{r} - n\right)\\ &= \sum_{k=n}^{2N_\mathrm{r}-n} \binom{2N_\mathrm{r}}{k} \prod_{l=1}^{k} \mathbb{P}\left(\mathrm{sign}(g_{i,l}) \ne \mathrm{sign}(g_{j,l})\right)\\ &\qquad \times \prod_{l=k+1}^{2N_\mathrm{r}} \mathbb{P}\left(\mathrm{sign}(g_{i,l}) = \mathrm{sign}(g_{j,l})\right). \quad (38)\end{aligned}$$

Let $u_{i,j,l} = \frac{g_{i,l}+g_{j,l}}{2}$, $v_{i,j,l} = \frac{g_{i,l}-g_{j,l}}{2}$, and $\delta_{i,j} = \|\mathbf{x}_i - \mathbf{x}_j\|_0$ be the number of different elements between two symbol vectors $\mathbf{x}_i$ and $\mathbf{x}_j$. Then the distributions of $u_{i,j,l}$ and $v_{i,j,l}$ are given by

$$u_{i,j,l} \sim \mathcal{N}\left(0, \frac{N_\mathrm{t} - \delta_{i,j}}{2}\right), \text{ and } v_{i,j,l} \sim \mathcal{N}\left(0, \frac{\delta_{i,j}}{2}\right), \quad (39)$$

for all $l \in \{1, \ldots, 2N_\mathrm{r}\}$. From (39) and the definitions of $u_{i,j,l}$ and $v_{i,j,l}$, we obtain

$$\begin{aligned}&\mathbb{P}\left(\mathrm{sign}(g_{i,l}) = \mathrm{sign}(g_{j,l})\right)\\ &= \mathbb{P}\left(\mathrm{sign}(u_{i,j,l} + v_{i,j,l}) = \mathrm{sign}(u_{i,j,l} - v_{i,j,l})\right)\\ &= \int_{-\infty}^{\infty} \frac{1}{\sqrt{\pi(N_\mathrm{t} - \delta_{i,j})}} e^{-\frac{u^2}{N_\mathrm{t}-\delta_{i,j}}} \int_{-|u|}^{|u|} \frac{1}{\sqrt{\pi\delta_{i,j}}} e^{-\frac{v^2}{\delta_{i,j}}} dv du\\ &= \frac{2}{\pi}\arctan\left(\sqrt{\frac{N_\mathrm{t} - \delta_{i,j}}{\delta_{i,j}}}\right) = p_{\mathrm{eq},\delta_{i,j}}. \quad (40)\end{aligned}$$

Substituting (40) into (38) and then applying the result to (36) yields (32). This completes the proof. ∎

As explained in Proposition 2, the exact CCDF of d_min is very complicated for the general number of the transmit antennas. When $N_\mathrm{t} = 2$, however, it is possible to derive the exact CCDF of d_min as follows:

Corollary 1. *When $N_\mathrm{t} = 2$, the exact CCDF of d_min is*

$$\mathbb{P}\left(d_\mathrm{min} \ge n\right) = \sum_{k=n}^{2N_\mathrm{r}-n} \binom{2N_\mathrm{r}}{k} 2^{-2N_\mathrm{r}}. \quad (41)$$

Proof: When $N_\mathrm{t} = 2$, the equation in (35) simplifies to

$$\mathbb{P}\left(d_\mathrm{min} \ge n\right) = \mathbb{P}\left(n \le \|Q(\mathbf{H}\mathbf{x}_1) - Q(\mathbf{H}\mathbf{x}_2)\|_0 \le 2N_\mathrm{r} - n\right). \quad (42)$$

Because $\delta_{1,2} = 1$, substituting both (38) and (40) into (42) yields

$$\begin{aligned}&\mathbb{P}\left(d_\mathrm{min} \ge n\right)\\ &= \sum_{k=n}^{2N_\mathrm{r}-n} \binom{2N_\mathrm{r}}{k} \left(\frac{2}{\pi}\arctan(1)\right)^{2N_\mathrm{r}-k} \left(1 - \frac{2}{\pi}\arctan(1)\right)^{k}\\ &= \sum_{k=n}^{2N_\mathrm{r}-n} \binom{2N_\mathrm{r}}{k} 2^{-2N_\mathrm{r}}. \quad (43)\end{aligned}$$

This completes the proof. ∎

One interesting observation from Corollary 1 is that the maximum possible value of d_min is N_r, which agrees with our intuition. To clearly see how d_min increases as a function of N_r, we also provide the following corollary:

Corollary 2. *When $N_\mathrm{t} = 2$, the probability that d_min is larger than $n = cN_\mathrm{r}$ asymptotically goes to 1, for any $0 \le c < 1$, i.e.,*

$$\lim_{N_\mathrm{r}\to\infty} \mathbb{P}\left(d_\mathrm{min} \ge cN_\mathrm{r}\right) = 1. \quad (44)$$

Proof: Theorem 5.3.2 in [24] says that for $0 \le t \le m$,

$$\sum_{k=0}^{m-t-1} \binom{2m}{k} 2^{-2m} + \sum_{k=m+t+1}^{2m} \binom{2m}{k} 2^{-2m} \le \exp\left(-\frac{t^2}{m+t}\right), \quad (45)$$

where m is a positive integer. Because $\sum_{k=0}^{2N_\mathrm{r}} \binom{2N_\mathrm{r}}{k} 2^{-2N_\mathrm{r}} = 1$, applying the above inequality to (41) yields

$$\mathbb{P}\left(d_\mathrm{min} \ge n\right) \ge 1 - \exp\left(-\frac{(N_\mathrm{r} - n)^2}{2N_\mathrm{r} - n}\right). \quad (46)$$

Let $n = cN_\mathrm{r}$ for any $0 \le c \le 1$. Then the lower bound of (46) becomes

$$\mathbb{P}\left(d_\mathrm{min} \ge n\right) \ge 1 - \exp\left(-\frac{(c-1)^2}{2-c} N_\mathrm{r}\right). \quad (47)$$

Except for $c = 1$, the RHS of the above inequality goes to 1 as N_r increases, so we obtain the results in (44). ∎

As we expected in Section V-A, Corollary 2 shows that for a sufficiently large N_r, $d_\mathrm{min} = N_\mathrm{r}$ with high probability. In this case, the symbol-vector-error probability exponentially decreases as N_r increases.

VI. Numerical Results

In this section, we provide simulation results to evaluate the performance of the proposed blind detection techniques compared to existing detection techniques, for the MIMO system with low-resolution ADCs. Furthermore, we validate the analysis given in Section V, by simulations.

A. SER of the Proposed Detection Techniques

In this subsection, we compare the SERs of the proposed and conventional detection techniques by using Monte Carlo simulations. In the simulations, we consider a MIMO system with low-resolution ADCs that use the uniform scalar quantizer defined in (2) with $\Delta = 0.5$. Channels are modeled as Rayleigh fading, so each element of the channel matrix is drawn from an IID circularly-symmetric complex Gaussian random variable with zero mean and unit variance. The lengths of the training phase and the data-transmission phase are selected as $T_\mathrm{t} = \frac{3}{2}K$ and $T_\mathrm{d} = \max\{9T_\mathrm{t}, 500 - T_\mathrm{t}\}$, respectively. We use the efficient channel-training method in Section IV-A, with $L = 3$. We apply the pilot-power-boosting assumption, so the SNR during the training phase is set to be 3-dB higher than the SNR operating for the data transmission.

We consider the following existing detection techniques for the purpose of the performance comparison.

- **Perfect CSIR, one-bit MLD**: ML detection (MLD) in [14], defined for one-bit ADCs, is used as a detection method when the channel matrix $\mathbf{H}$ is perfectly known at the receiver. This technique achieves the upper bound of the SER for the one-bit-ADC case.

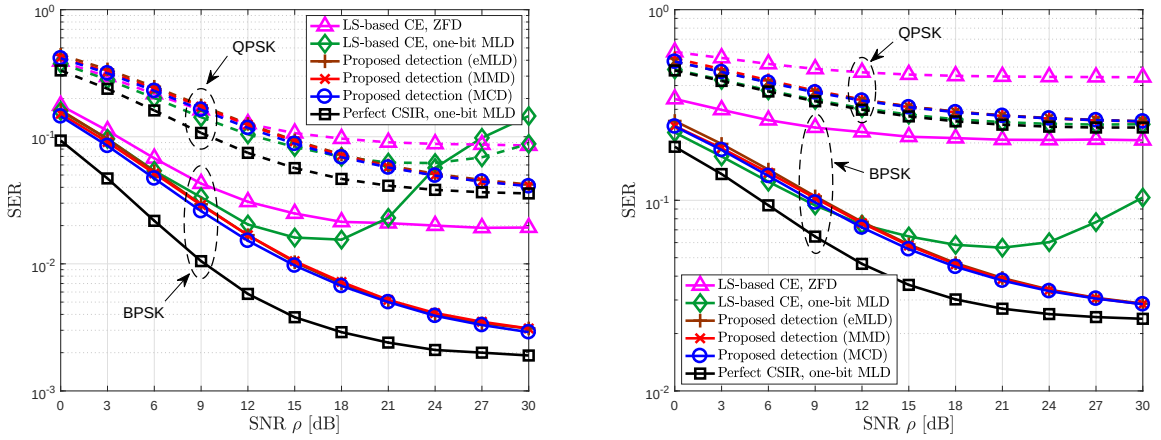

(a) $(N_{\rm t}, N_{\rm r}) = (2, 4)$ case (b) $(N_{\rm t}, N_{\rm r}) = (4, 4)$ case

Fig. 4. SER vs. SNR of the proposed and conventional detection techniques for MIMO systems with one-bit ADCs for BPSK and QPSK modulation.

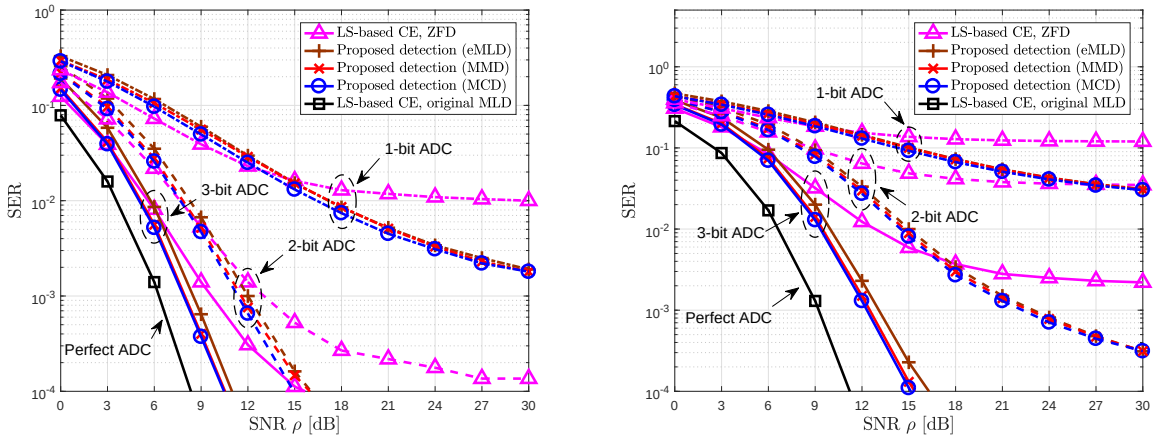

(a) $(N_{\rm t}, N_{\rm r}) = (2, 8)$ case (b) $(N_{\rm t}, N_{\rm r}) = (4, 8)$ case

Fig. 5. SER vs. SNR of the proposed and conventional detection techniques for various numbers of ADC bits when employing QPSK modulation.

- **LS-based CE, one-bit MLD**: MLD in [14], defined for one-bit ADCs, is used as a detection method when the channel matrix $\mathbf{H}$ is estimated based on an LS method that uses pilot signals of length $T_{\rm t}$.
- **LS-based CE, original MLD**: Original MLD for perfect-ADC case is used as a detection method when the channel matrix $\mathbf{H}$ is estimated based on an LS method that uses pilot signals of length $T_{\rm t}$.
- **LS-based CE, ZFD**: Zero-forcing-type detection (ZFD) in [14] is used as a detection method when the channel matrix $\mathbf{H}$ is estimated based on an LS method that uses pilot signals of length $T_{\rm t}$.

Note that the first two techniques are only applicable to one-bit ADCs, whereas the last two techniques are applicable regardless of the resolution of the ADCs.

Fig. 4 shows the SERs of the proposed and conventional detection techniques for the MIMO systems with the one-bit ADCs ($B = 1$). As SNR increases, the SERs of all proposed detection techniques converge to the SER upper bound achieved by the one-bit MLD with perfect CSIR, even when the training sequence is very short ($T_{\rm t} = 6$ for BPSK and $T_{\rm t} = 24$ for QPSK). Whereas, two conventional techniques that are based on channel estimation show severe SER degradation in most cases. This is because the accuracy of CSIR obtained by the channel-estimation method is inaccurate when the pilot length is insufficient and the quantization error at the ADC is high. Particularly, the proposed techniques outperform the one-bit MLD method with channel estimation, except in the limited region of high SER (SER > 0.1).

Fig. 5 shows the SERs of the proposed and conventional detection techniques for various numbers of ADC bits when employing QPSK modulation. It is observed that the proposed detection techniques provide a significant SER reduction as the number of ADC bits increases. Particularly, the ADC with 3-bit resolution is sufficient for the proposed techniques to achieve the SER near to the perfect-ADC case with channel estimation, whereas the conventional method (ZFD with channel estimation) still shows an error floor.

In both figures 4 and 5, three proposed detection methods show very similar SER performance for all antenna configu-

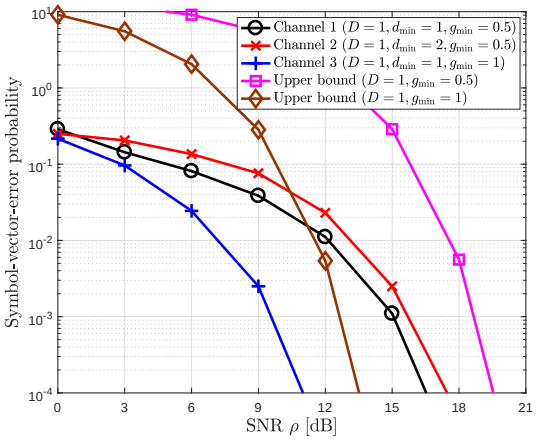
Channel 1 ($D=1, d_{\min}=1, g_{\min}=0.5$)
Channel 2 ($D=1, d_{\min}=2, g_{\min}=0.5$)
Channel 3 ($D=1, d_{\min}=1, g_{\min}=1$)
Upper bound ($D=1, g_{\min}=0.5$)
Upper bound ($D=1, g_{\min}=1$)
Symbol-vector-error probability
SNR ρ [dB]

Fig. 6. Comparison between the upper bound in (21) and the symbol-vector-error probability of MCD when $N_{\rm t}=2$ and $N_{\rm r}=2$.

rations and SNRs. Surprisingly, MCD outperforms the other two proposed methods even if it has the lowest detection complexity. Therefore, MCD is the most attractive detection method for use in practical MIMO systems with low-resolution ADCs. This superiority is possible because the empirical conditional PMFs are unreliable when the repetition number at the channel training is insufficient ($L=3$), whereas MCD is relatively insensitive to the unreliability of the empirical conditional PMFs. Although eMLD is guaranteed to be optimal for sufficiently large L, eMLD achieves the lower SER than MMD in simulations where $L=3$; this agrees with our expectation in Section IV-B.

B. Validation of Analysis

In this subsection, we compare the analysis results in Section V with the simulation results when the MIMO systems with the one-bit ADCs ($B=1$) and BPSK modulation are considered.

In Fig. 6, the upper bound in (21) is compared with the symbol-vector-error probability of MCD when $N_{\rm t}=2$ and $N_{\rm r}=2$. In the simulations, the one-bit ADCs use the uniform scalar quantizer defined in (2) with $\Delta=0.5$, and the lengths of the training phase and the data-transmission phase are selected as $T_{\rm t}=3K$ and $T_{\rm d}=10^5$, respectively. We use the efficient channel-training method in Section IV-A, with $L=6$. As in the previous subsection, we apply the power-boosting assumption on the SNR of the training phase. We conduct the simulations for three channel environments:

- **Channel 1:** A channel matrix is given by

$$\mathbf{H}_1=\begin{bmatrix}-1-\sqrt{-1} & 0\\ 1+0.5\sqrt{-1} & -\sqrt{-1}\end{bmatrix}, \tag{48}$$

  which satisfies $D=1$, $d_{\min}=1$, and $g_{\min}=0.5$.
- **Channel 2:** A channel matrix is given by

$$\mathbf{H}_2=\begin{bmatrix}0.5 & -1+0.5\sqrt{-1}\\ -1-1.5\sqrt{-1} & 0.5\end{bmatrix}, \tag{49}$$

  which satisfies $D=1$, $d_{\min}=2$, and $g_{\min}=0.5$.

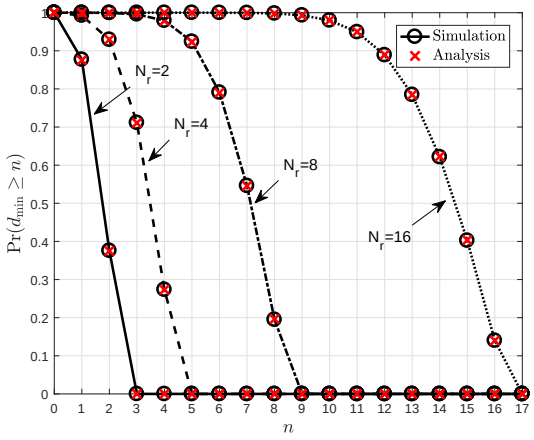

(a) $N_{\rm t}=2$

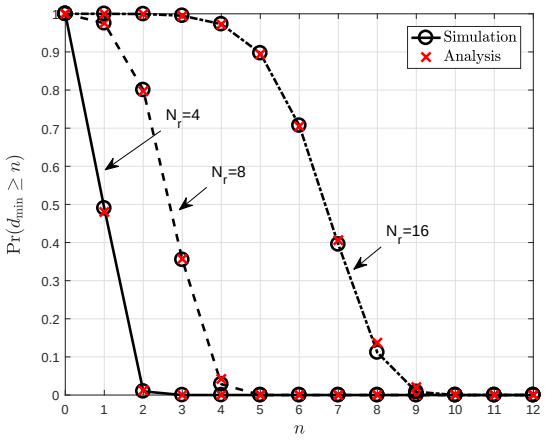

(b) $N_{\rm t}=4$

Fig. 7. Comparison between the analyzed and simulated CCDFs of $d_{\min}$ for various antenna configurations.

- **Channel 3:** A channel matrix is given by

$$\mathbf{H}_3=\begin{bmatrix}-1-\sqrt{-1} & 0\\ 1 & -\sqrt{-1}\end{bmatrix}, \tag{50}$$

  which satisfies $D=1$, $d_{\min}=1$, and $g_{\min}=1$.

Fig. 6 shows that all symbol-vector-error-probability curves are indeed lower than the corresponding upper bound calculated from the analysis. Particularly, although Channel 1 and 2 have different values of $d_{\min}$, their error curves have the same upper bound; this result coincides with the analysis results in (21), in which the upper bound of the symbol-vector-error probability is determined by D, not by $d_{\min}$. Furthermore, the decreasing order of the symbol-vector-error-probability curve is shown to be larger for Channel 1 ($g_{\min}=0.5$) than for Channel 3 ($g_{\min}=1$); this result also agrees with the results given in (21). The difference between the SNRs of the upper bound and MCD that achieve $P_{\rm e}^{\rm vec}=10^{-4}$ is less than 3 dB in all cases.

In Fig. 7, the CCDFs calculated using (32) and (41) are compared with the CCDF of $d_{\min}$ obtained from the simulations when $N_{\rm t}=2$ and $N_{\rm t}=4$, respectively. For $N_{\rm t}=2$, the analyzed and simulated CCDFs are almost the same regardless

of $N_{\rm r}$. Furthermore, for $N_{\rm t} = 4$, although the simulated CCDF is slightly different from the analyzed CCDFs, the difference is negligible. Therefore, these results validate the analysis given in Corollary 1 and Theorem 2. Another observation obtained from Fig. 7 is that the value of $d_{\min}$ is expected to increase as $N_{\rm r}$ increases; this result coincides with the intuition obtained from Corollary 2.

VII. Conclusion

In this paper, we have presented novel blind detection techniques for MIMO systems with low-resolution ADCs, inspired by supervised learning. The proposed techniques do not require explicit CSIR; instead they learn a nonlinear function that characterizes the input-output relation of the system, including the effects of the channel matrix and the quantization at the ADCs. For the one-bit ADCs and BPSK modulation, we have analyzed the symbol-vector-error probability of the proposed method, and have shown that the upper bound of this probability decreases exponentially with the minimum distance that can increase with the number of receive antennas. Simulations suggest that the proposed approach can be extended to MIMO systems that use ADCs with an arbitrary number of precision levels.

Although we have focused on single-user MIMO systems, it is also possible to apply the proposed approach to multi-user MIMO scenarios. It would also be interesting to investigate the impact on how non-uniform quantization methods affect the performance of the proposed methods as a future work.

References

[1] B. Murmann, "ADC performance survey 1997-2016," [Online]. Available: http://web.stanford.edu/∼murmann/adcsurvey.html

[2] R. H. Walden, "Analog-to-digital converter survey and analysis," *IEEE J. Sel. Areas Commun.*, vol. 17, no. 4, pp. 539–550, Apr. 1999.

[3] J. A. Nossek and M. T. Ivrlac, "Capacity and coding for quantized MIMO systems," in *Proc. IEEE Int. Wireless Commun. Mobile Computing Conf. (IWCMC)*, July 2006.

[4] J. Singh, O. Dabeer, and U. Madhow, "On the limits of communication with low- precision analog-to-digital conversion at the receiver," *IEEE Trans. Commun.*, vol. 57, no. 12, pp. 3629–3639, Dec. 2009.

[5] O. Dabeer and U. Madhow, "Channel estimation with low-precision analog-to-digital conversion," in *Proc. IEEE Int. Conf. Commun. (ICC)*, May 2010.

[6] J. Mo and R. W. Heath, Jr., "Capacity analysis of one-bit quantized MIMO systems with transmitter channel state information," *IEEE Trans. Signal Process.*, vol. 63, no. 20, pp. 5498–5512, Oct. 2015.

[7] N. Liang and W. Zhang, "Mixed-ADC massive MIMO," *IEEE J. Sel. Areas Commun.*, vol. 34, no. 4, pp. 983–997, Apr. 2016.

[8] C. Mollen, J. Choi, E. G. Larsson, and R. W. Heath, Jr., "One-bit ADCs in wideband massive MIMO systems with OFDM transmission," in *Proc. IEEE Int. Conf. on Acoust., Speech and Signal Process. (ICASSP)*, Mar. 2016.

[9] J. Choi, D. J. Love, D. R. Brown, III, and M. Boutin, "Quantized distributed reception for MIMO wireless systems using spatial multiplexing," *IEEE Trans. Signal Process.*, vol. 63, no. 13, pp. 3537–3548, July 2015.

[10] S. Jacobsson, G. Durisi, M. Coldrey, U. Gustavsson, and C. Studer, "One-bit massive MIMO: Channel estimation and high-order modulations," in *Proc. IEEE Int. Conf. Commun. (ICC)*, June 2015.

[11] S. Wang, Y. Li, and J. Wang, "Multiuser detection in massive spatial modulation MIMO with low-resolution ADCs," *IEEE Trans. Wireless Commun.*, vol. 14, no. 4, pp. 2156–2168, Apr. 2015.

[12] C.-K. Wen, C.-J. Wang, S. Jin, K.-K. Wong, and P. Ting, "Bayes-optimal joint channel-and-data estimation for massive MIMO with low-precision ADCs," *IEEE Trans. Signal Process.*, vol. 64, no. 10, pp. 2541–2556, May 2016.

[13] S.-N. Hong, Y.-S. Jeon, and N. Lee, "MIMO systems with low-resolution ADCs: Linear coding approach," *submitted to IEEE Trans. Wireless Commun.*, 2016.

[14] J. Choi, J. Mo, and R. W. Heath, Jr., "Near maximum-likelihood detector and channel estimator for uplink multiuser massive MIMO systems with one-bit ADCs," *IEEE Trans. Commun.*, vol. 64, no. 5, pp. 2005–2018, May 2016.

[15] J. Mo, P. Schniter, N. G. Prelcic, and R. W. Heath, Jr., "Channel estimation in millimeter wave MIMO systems with one-bit quantization," in *Proc. IEEE Asilomar Conf. Signals Syst. Comput.*, Nov. 2014, pp. 957–961.

[16] Y. Li, C. Tao, G. Seco-Granados, A. Mezghani, A. L. Swindlehurst, and L. Liu, "Channel estimation and performance analysis of one-bit massive MIMO systems," arXiv:1609.07427 [cs.IT], Sep. 2016. [Online]. Available: http://arxiv.org/abs/1609.07427

[17] L. Zheng and D. N. C. Tse, "Communication on the Grassmann manifold: A geometric approach to the noncoherent multiple-antenna channel," *IEEE Trans. Inf. Theory*, vol. 48, no.2, pp. 359–383, Feb. 2002.

[18] L. Tong, G. Xu, and T. Kailath, "Blind identification and equalization based on second-order statistics: A time domain approach," *IEEE Trans. Inf. Theory*, vol. 40, no.2, pp. 340–349, Mar. 1994.

[19] H. Bolcskei, R. W. Heath, Jr., and A. J. Paulraj, "Blind channel estimation in spatial multiplexing systems using non redundant antenna precoding," in *Proc. IEEE Asilomar Conf. Signals Syst. and Comput.*, 1999, pp. 1127–1132.

[20] M. Abuthinien, S. Chen, and L. Hanzo, "Semi-blind joint maximum likelihood channel estimation and data detection for MIMO Systems," *IEEE Signal Process. Lett.*, vol. 15, pp. 202–205, 2008.

[21] S. Chen, S. Sugiura, and L. Hanzo, "Semi-blind joint maximum likelihood channel estimation and data detection for MIMO Systems," *IEEE Signal Process. Lett.*, vol. 17, no. 12, pp. 993–996, Dec. 2010.

[22] H.-W. Liang, R. Y. Chang, W.-H. Chung, and S.-Y. Kuo, "A reduced-complexity blind detector for MIMO system using K-means clustering algorithm," in *Proc. IEEE Veh. Tech. Conf. (VTC) Spring*, June 2013.

[23] A. Schenk and R. F. H. Fischer, "Noncoherent detection in massive MIMO systems," in *Proc. Int. ITG Workshop Smart Antennas (WSA)*, Mar. 2013.

[24] L. Lovász, J. Pelikán, and K. Vesztergombi, *Discrete mathematics: Elementary and beyond*, New York, NY, USA: Springer, 2003.